Environ Res Tec, Vol. 7, Issue. 3, pp. 406–421, September 2024

Environmental Research and Technology
https://ert.yildiz.edu.tr - https://dergipark.org.tr/tr/pub/ert
DOI: https://10.35208/ert.1443393

Environmental Research & Technology

Research Article

Investigating the emissions and performance of ethanol and biodiesel blends on Al_2O_3 thermal barrier coated piston engine using response surface methodology design - multiparametric optimization

P. KUMARAN[*,1], S. NATARAJAN SENGODAN[2], Sudesh KUMAR MP.[3], A. ANDERSON[4], S. PRAKASH[5]

[1]*Department of Mechanical Engineering, Aarupadai Veedu Institute of Technology, Vinayaka Mission's Research Foundation, Deemed to be University, Tamil Nadu, India*
[2]*Vinayaka Missions Kirupananda Variyar Engineering College, Vinayaka Mission's Research Foundation, Salem, Tamil Nadu, India*
[3]*Department of Mechanical Engineering, Global Institute of Engineering and Technology, Tamil Nadu, India*
[4]*School of Mechanical Engineering, Sathyabama Institute of Science and Technology, Chennai, India*
[5]*Department of Mechanical Engineering, Aarupadai Veedu Institute of Technology, Vinayaka Mission's Research Foundation, Deemed to be University, Tamil Nadu, India*

ARTICLE INFO

Article history
Received: 27 February 2024
Revised: 22 March 2024
Accepted: 01 April 2024

Key words:
Emission; Ethanol; Optimization; Performance; Thermal barrier coating; Tomato methyl ester

ABSTRACT

The Response Surface Methodology (RSM) optimization technique was used to examine the effect of load, Tomato Methyl Ester (TOME), and Ethanol injection enhanced diesel on engine performance and exhaust gas emissions with a normal piston and an Al_2O_3 coated piston. TOME biodiesel (10, 20, and 30%) and ethanol (10, 20, and 30%) were chosen to increase BTE while minimizing BSFC, NOx, CO, smoke, and HC. The RSM technique was used to operate the engine by load (0–100%). The results revealed that engine load, TOME, and ethanol concentration all exhibited a considerable effect on the response variables. The ANOVA results for the established quadratic models specified that for each model, an ideal was discovered by optimizing an experiment's user-defined historical design. The present research efforts to improve the performance of a diesel engine by using a thermal barrier-coated piston that runs on biodiesel blends. Al_2O_3 is the chosen material for TBC due to its excellent thermal insulation properties. B20E30 has a 4% higher brake thermal efficiency than diesel, but B10E20 and B30E20 mixes have a 3.6% and 12% reduction in BSFC. The B20 blends lowered CO and HC emissions by 6% and 8% respectively. In terms of performance and emissions, biodiesel blends performed similarly to pure diesel, and the combination was optimized through the design of an experiment tool.

Cite this article as: Kumaran P, Natarajan Sengodan S, Kumar SMP, Anderson A, Prakash S. Investigating the emissions and performance of ethanol and biodiesel blends on Al_2O_3 thermal barrier coated piston engine using response surface methodology design - multiparametric optimization. Environ Res Tec 2024;7(3)406–421.

***Corresponding author.**
*E-mail address: kumaranp@avit.ac.in

INTRODUCTION

The application of piston TBC is highly beneficial in mini-mizing heat dissipation during the operation of an internal combustion engine's process. Total combustion is hindered throughout the process of combustion due to multiple factors. The loss of warmth in the combustion cylinder is a contributing factor to incomplete combustion. The primary objective of piston TBC is not alone to prevent heat loss, but also to pro-vide fatigue protection and reduce emissions. This research aims to mitigate engine heat loss by applying a TBC material on the piston, specifically using copper-chromium-zirconium (CuCr1Zr) [1]. The application of CuCr1Zr as a TBC material on pistons is an innovative method that has been evaluated using Tamanu mixed diesel fuel [2]. An examination was con-ducted on an IC engine that had a coating applied to it, the piston was coated using the plasma spray technique with a layer of Ni-Cr measuring 0.2 mm in thickness [3]. Mamey sapote oil was utilized as a source of biodiesel. Consequently, there was a 1% improvement in thermal efficiency, accompanied by a decrease in (CO) emissions [4]. A study was di-rected to evaluate the act of a single cylinder IC engine with copper coating [5]. The findings shown that the implementation of a Cu-coated piston and combustion chamber in the engine effectively decreases the levels of (HC) and (CO) emissions [6]. Conducted research on the impact of plasma sprayed zirconium coatings on the piston. One effective method for enhancing the performance of internal combustion engines and decreasing the emission of (CO) and hydrocarbons (HC) is the use of thermal barrier coatings on the piston and combustion chamber [7]. Declared that a diesel engine with a coating exhibits superior performance [8]. It has been asserted that cotton seed biodiesel can serve as a substitute fuel to regulate the pollutants, such as carbon monoxide (CO) and hydrocarbons (HC), produced by a diesel engine [9]. It was asserted that cotton seed biodiesel was employed as a substitute fuel to regulate the emissions of carbon monoxide (CO) and hydrocarbons (HC) from a diesel engine [10]. The combustion parameters have an impact on power generation, emission of pollutants from the exhaust, fuel consumption, engine vibrations, and noise levels [11]. Coating cylinders and adding nanoparticles to biodiesel reduce fuel consumption [12] Compressed air's pressure and temperature affect how long it takes to ignite. During compression, the cooling system effectively absorbs a significant quantity of heat. Engines equipped with thermal barrier coatings can reduce heat dissipation and improve the effective output by employing materials with low thermal conductivity and high resilience to high temperatures to cover the combustion chambers [13, 14]. A zirconia coating is applied to engine components, which results in a reduction in the heat conduction of such components [15]. Furthermore, the utilization of a glow plug in conjunction with the utilization of ethanol as a fuel consequences in a discount in the emission of pollutants emitted by exhaust [16, 17]. On the other hand, as compared to the utilization of diesel fuel, it results in a decrease in efficiency. SVM and Bagging methods perform second-best for Cp max and smoke output variables, respectively [18]. On the other hand, there is a certain degree of improvement in the thermal efficiency of the engine when the timing of injection is delayed [19]. This results in a reduction in emissions of CO_2 and hydrocarbons that have not been burned, as well as an improvement in thermal efficiency [20]. In spite of this, it outcomes in an increase in the amount of nitrogen oxide emissions since it causes the combustion temperatures to rise [21]. As a result of their improved thermal and mechanical efficiency, fewer pollutant emissions, and decreased fuel consumption, thermal barrier coatings have become increasingly prevalent in engine components. The waste heat created by the engine's insulation can be harnessed to oxidize the soot precursors generated during hydrocarbon combustion, leading to a reduction in emissions [22]. Exhaust emissions decreased with the addition of Di Ethylene Butyl Glycol Ether [23]. Table 1 show the literature based on various biodiesel.

Table 1. Literature on different biodiesel and methods

Author	Oil used	Methods	Result
A. P. Venkatesh [1]	Rubber seed biodiesel	Ethanol additive, nanocoated pistons, optimization	A biodiesel-compatible thermal barrier-coated piston improves diesel engine performance in the study. Thermal insulation makes yttria-stabilized zirconia appropriate for thermal barrier coatings.
Saxena [5]	Acacia Concinna	Response surface methodology, nanofluid	TiO_2 nanoparticle-enhanced Acacia Concinna biodiesel-diesel blends improve engine performance; BTE, BSFC, ID, HC, and smoke emissions decrease; NOx emissions increase.
Salih Ozer [12]	Coalbed methane	Nanoparticle (molybdenum) additive, coated pistons	Al_2O_3 + 13% TiO_2 coating tractor engine cylinders and adding molybdenum nanoparticles to biodiesel reduced fuel consumption, HC, CO, PM, exhaust gas temperature, and NOx emission.
Viswanathan [20]	Pine oil	Thermal barrier coating and antioxidants	Pine oil biofuel was utilized to test diesel engine with thermal barrier and antioxidants. PO+TBHQ combination gave the best performance, combustion, and emissions, suggesting engine efficiency and pollution reduction.
Mejia et al. [15]	Castor oil biodiesel, palm oil bio diesel	Dual Biodiesel, Compression ratio	It was not a viable alternative to use blends of palm oil biodiesel and castor oil biodiesel (POB COB) in order to generate a sort of pure biodiesel that had a low cloud point and a low viscosity.

The objective of this research is to describe the use of the (RSM) optimization technique in examining the impact of load, Tomato Methyl Ester (TOME), and Ethanol injection on engine performance and exhaust gas emissions. The main aims to highlight the experimental design, factors considered (TOME and Ethanol concentrations), and the use of RSM for optimization. The goal of the paragraph is to present research efforts focused on improving the performance of a diesel engine using biodiesel blends. It introduces the application of a TBC piston running on biodiesel blends, specifically B20E30, B10E20, and B30E20, and compares their performance and emissions with pure diesel. The use of Al_2O_3 as the material for thermal barrier coatings is mentioned, and the overall aim is to maximize (BTE), minimize (BSFC), and reduce NOx, CO, smoke, and HC emissions.

MATERIALS AND METHODS

Tomato Methyl Ester Formation

Tomato seeds are not commonly used for biodiesel production due to their relatively low oil content in comparison to other oilseed crops like soybeans or canola. Nevertheless, the wastage of seed extracted from sauce factory within the scope of investigating the creation of biodiesel from non-traditional sources, below is a comprehensive outline of the biodiesel manufacturing procedure, commonly referred to as transesterification. Figure 1 shows the Tomato seed oil extraction: Obtain oil from tomato seeds. Typically, this procedure involves either mechanical pressing or solvent extraction. The oil concentration in tomato seeds is quite modest in comparison to specialized oilseed crops, thus potentially limiting the production. Oil Refining: Purify the produced oil if necessary. The enhancement of oil quality can be achieved through several refining techniques such as degumming, neutralization, bleaching, and deodorization. Transesterification: Convert the purified oil into biodiesel using the process of transesterification. The process of chemically interacting vegetable oil or animal fat with an spirits, characteristically methanol or ethanol, in the occurrence of a catalyst, typically sodium or potassium hydroxide [23]. This process transforms the triglycerides present in the oil into esters, which are commonly known as biodiesel, as well as glycerol. Separation and Washing: Following the transesterification process, the biodiesel should be separated from the glycerol and subjected to a washing procedure in order to eliminate any contaminants. Dehydration: from the biodiesel by the process of drying. Table 2 shows the chemical properties.

TBC – Before & After Piston Crown

Following the application of the TBC, the piston crown is depicted in Figure 2: According to the findings of the research analysis, the materials that are utilized for thermal barrier coating include NicrAl, Al_2O_3, molybdenum, titanium oxide, Yttrium stabilized zirconium, magnesium stabilized zirconia, and other similar substances.

Table 2. Properties of fuels

Properties	TME	Diesel	Ethanol
Viscosity (cSt)	28	2.62	1.52
Flashpoint (°C)	189	68	13
Calorific value (MJ/kg)	35.9	42.7	27.3
Density (kg/m^3)	915.1	855	720

TME: Tomato methyl ester.

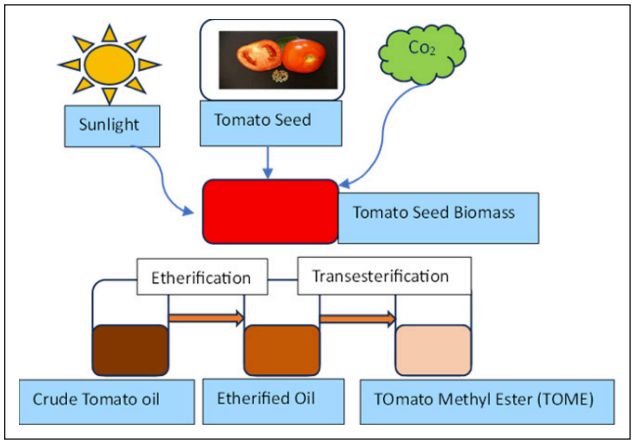

Figure 1. Preparation of tomato methyl ester.

The simplified chemical reaction is as follows: Triglyceride + Alcohol → Biodiesel + Glycerol

Figure 2. Piston before/after coating.

The barrier coating that was used for this work was a piston-based coating with NiCr – 80 (Micron), Top Piston Crown Al_2O_3-100, and Total TBC – 180 (Microns). As a covering material, the ceramic material known as "Aluminum oxide" was utilized for the piston crown associated with the diesel engine. There are a number of vital features that the artistic material must possess, including strong thermal conduction, good mixing, wear fence, and from top to bottom heat shock resistance. There was a shielding thermal barrier that was placed above the piston crown. With the use of the plasma splash technique, the substance Al203 that had been fired was coated over the substratum to a thickness of 200 µm [24]. All of the experimental work on the piston crown has been finished, as shown in Figure 3.

Figure 3. Experimental work on piston crown.

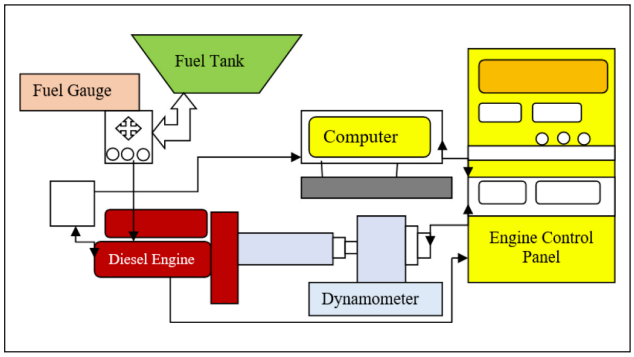

Figure 4. Experimental setup.

Figure 5. Experimental setup of VCR diesel engine (photographic view).

Uncertainty Analysis

Visualization, range, devices, atmosphere, and calibration were used to estimate error as well as uncertainty evaluation, which was then split down into assigned and fixed errors by process time. For accurate results, undertake an uncertainty analysis. The transfer of uncertainty technique, or root mean square, was used to assess engine systems uncertainty. The equation (1) was used to analyze engine efficiency parameter uncertainty.

$$\varphi_R = \left[\left(\frac{\partial R}{\partial x_1}\varphi_1\right)^2 + \left(\frac{\partial R}{\partial x_2}\varphi_2\right)^2 + \cdots + \left(\frac{\partial R}{\partial x_n}\varphi_n\right)^2\right]^{\frac{1}{2}} \quad (1)$$

Experimental Setup

A kirloskar engine single chamber, four strokes, and an engine which links are connected to the control panel make up the design illustrated in Figure 4. Figure 5 illustrated the photographic view of experimental engine; The load can range from 0 to 5.2 KW according to the arrangement. In instruction to facilitate reading, the power output of the engine is 5.2 kilowatts when it is operating at 0 percent load, 50% load, and 100% full load. In the fuel container, the air mixture with fuel that is used with diesel and biodiesel is permitted, and the amount of the combination of fuels is controlled by the fuel calculator that is located on the control panel. The smoke meter and inlet manifold are some of the other configurations that may be programmed due to the open digital control panel. Sensors such as the fuel sensor, level sensor and load sensor, are monitored on (ECUs) and data analytics devices [25]. The engine specifications for the test engine are listed in Table 3.

Experimental Design

The trial design, optimization, and validation processes have all been carried with the support of the Design-Expert® application, version 13. In the Table 4, the data input factors and

Table 3. Specifications of test engine

Make	Kirloskar, 4S
No. of cylinder	One
Bore	87.5 millimeter
Stroke	110 millimeter
Power	5.2 kilo watt
Compression ratio	17.5:1
Speed	1500 rpm
Fuel injection timing	23o b TDC
Injection pressure	200 bars

their respective levels are presented. A numerical calculation is performed on each and every variable that is entered. In order to maximize BTE while simultaneously improving BSFC, and diminishing NOx, CO, smoke, and HC, the load was selected to be between 0 and 100%, the TOME mix biodiesel (10, 20 and 30%), and the ethanol (10, 20 and 30%).

In the process of developing quadrat-ic and Box-Behnken models of estimation for inputs and response variables, RSM is a method of analysis that is generally utilized. RSM is helpful in assessing the influence that input parameters have on response variables, reducing the number of trials that are conducted, and maximizing the effectiveness of response variables. The experimental setup

Table 4. Factors and levels for TOME Blends with ethanol and load

Process parameters	Levels		
	1	2	3
A- Load (KG)	0	50	100
B- TOME blend (%)	10	20	30
C- Ethanol (%)	10	20	30

TME: Tomato methyl ester.

matrix for tomato methyl ester blends mixed with ethanol and load (in kilograms) is presented in Table 5. The result is obtained for the Normal Piston and Thermal Barrier (Al_2O_3) Coated Piston.

RESULT AND DISCUSSION

Exhibited values of R2, Adj. R2, Pred. R2, and a suitable precise appropriate within the required constraints for precision and adequate of the model for aimed responses are presented here, along with a summary of the analysis of variance (Table 6 for Normal piston and Table 7 for coated piston) and a review of the models for the performance of the normal piston and the Al_2O_3 coating piston in BTE and BSFC. Additionally, the presented data includes the emission characteristics of CO, HC, NoX, and smoke.

Table 5. Experimental design matrix for load/TOME/ethanol – normal & Al2O3 piston

Sl. No	Load (kg)	TOME (%)	Ethanol (%)	Normal piston						Thermal barrier (Al_2O_3) coated piston					
				BTE	BSFC	CO	HC	NoX	Smoke	BTE	BSFC	CO	HC	NoX	Smoke
1	50	30	30	29	0.27	0.02	55	540	3.8	30.5	0.66	0.038	52.7	385.4	18.9
2	0	20	30	19	0.67	0.02	45	797	6	31.5	0.39	0.108	50.6	568.1	38.2
3	50	20	20	28	0.4	0.01	48	398	11	30	0.28	0.036	50.2	529.4	23.8
4	50	20	20	31	0.29	0.09	45	573	23	27	0.23	0.039	39.8	762.9	18.6
5	100	20	30	32	0.24	0.01	48	560	17	25	0.65	0.046	56.5	395.8	10.7
6	50	10	10	30	0.66	0.02	35	755	4.5	19	0.39	0.117	54.4	578.5	30
7	50	20	20	31.6	0.4	0.01	45	367	5.6	15	0.3	0.045	53.9	539.8	15.6
8	0	30	20	30	0.31	0.08	49	528	10	14	0.25	0.047	43.6	773.3	10.42
9	50	30	10	27.5	0.26	0.02	41	494	28	21	0.2	0.031	50.8	400.4	7.76
10	100	30	20	25	0.21	0.02	37	752	14.2	23	0.66	0.102	48.7	583.1	27
11	0	20	10	19	0.67	0.04	44	638	5.5	28.5	0.67	0.03	48.3	544.4	12.67
12	100	20	10	15.4	0.68	0.01	47	662	28.5	15	0.7	0.032	37.9	777.9	7.48
13	100	10	20	14	0.71	0.005	40	686	19	25	0.3	0.04	54.6	364	8.33
14	0	10	20	21	0.46	0.03	52	659	4.15	29	0.67	0.11	52.5	546.7	27.6
15	50	20	20	23	0.34	0.11	58	258	18.5	19	0.42	0.038	52	508	13.25
16	50	20	20	28.5	0.31	0.025	45	536	19	28	0.32	0.041	41.7	741.5	8.05
17	50	10	30	15	0.68	0.08	63	343	12.5	31	0.45	0.054	46.6	658.4	21

BTE: Brake thermal efficiency; BSFC: Brake-specific fuel consumption.

Table 6. Test of hypotheses for BSFC, BTE, CO, HC, NoX, and smoke as predictor variables for normal piston

	Normal piston					
	BTE (%)	**BSFC (kg/kW-h)**	**CO (% vol)**	**HC (ppm)**	**NoX (ppm)**	**Smoke (BSU)**
Standard deviation	6.69	0.2091	0.0330	6.91	138.47	8.61
Mean	24.65	0.4447	0.0353	46.88	561.53	13.54
C.V. %	27.14	47.02	93.50	14.74	24.66	63.59
R^2	0.4989	0.4593	0.5612	0.5952	0.6482	0.5229
Adjusted R^2	-0.1453	-0.2359	-0.0030	0.0748	0.1958	-0.0906
Predicted R^2	-4.6141	-4.8640	-2.5474	-4.0777	-1.0519	-2.4841
Adeq precision	3.4768	3.2113	3.4076	3.9860	3.9806	3.4070

BTE: Brake thermal efficiency; BSFC: Brake-specific fuel consumption.

Table 7. Test of hypotheses for BSFC, BTE, CO, HC, NoX, and smoke as predictor variablesfor Al_2O_3 coated piston

	Thermal barrier (Al_2O_3) coated piston					
	BTE (%)	**BSFC (kg/kW-h)**	**CO (% vol)**	**HC (ppm)**	**NoX (ppm)**	**Smoke (BSU)**
Standard deviation	5.55	0.1927	0.0326	4.71	138.65	10.24
Mean	24.21	0.4435	0.0561	49.11	568.09	17.61
C.V. %	22.94	43.45	58.14	9.59	24.41	58.14
R^2	0.6259	0.5154	0.5179	0.6762	0.5550	0.4531
Adjusted R^2	0.1449	-0.1075	-0.1020	0.2600	-0.0171	-0.2500
Predicted R^2	-0.4493	-3.1506	-1.5571	-1.2407	-3.0634	-1.9570
Adeq precision	4.1089	3.4164	3.4715	5.0048	4.1483	2.9339

BTE: Brake thermal efficiency; BSFC: Brake-specific fuel consumption.

The outcomes of the experiment were subjected to (ANOVA), and a number of models were created in the design expert. The projected values were then calculated using the equations. Therefore, in order to determine the most desirable parameter configurations, acceptability analysis was applied using the direct equation for getting better results.

Performance Result

Equation 2 for a Normal Piston and Equation 3 for an Al_2O_3 Coated Piston were derived from the RSM quadratic model of BTE based on the measured parameters.

[BTE=27.82+-1.075*A+-2.3125*B+-0.3875*C+-4.25*AB+-0.9AC+4.625*BC+-3.0475*A^2+-3.5225*B^2+-0.1725*C^2] (2)

[BTE=26.8+-2.75*A+-1.5625*B+1.4375*C+-0.5*AB+-6AC+0.375*BC+-5.0875*A^2+-1.2125*B^2+0.7875*C^2] (3)

Figure 6 (a) 2D and (b) 3D surface plot shows the BTE performance of normal piston, the impact of the quadratic factors Initialize, TOME Mix with the addition of ethanol infusion When subjected to the highest possible load circumstances, the (BTE) of B20E30 was determined to be around 4% more than that of pure diesel. Increased the amount of oxygen in ethanol enhances its combustion efficiency, leading to heightened thermal performance [26, 27]. Due to the increased viscosity and subsequent decrease in combustion rate coming from the elevated ethanol concentration in the mixture, the (BTE) is lower compared to B10E20, as shown in Table 6. As the ethanol concentration in the fuel blend improves, the TE of the brakes enhances. The outside temperature of the combination of air and fuel drops as the ethanol energy share increases because of the heat that ethanol absorbs and its high volatility. This is because they create an increase in the blend density, which in turn causes the temperature to decrease. In comparison to previous engines, the low heat rejection engine, which was fitted with a fully stabilised Al_2O_3 coating, demonstrated a higher level of thermal efficiency.

This can be ascribed to the ceramics coating's ability to act as a heat barrier, which effectively separates the engine from the environment around it. The B20E30 blend exhibited an approximately 3.5% increase in comparison to pure diesel, however its (BTE) was lower than that of the B30E20 blend [12]. Minimizing heat dissipation enables a boost in engine output and thermal effectiveness which shown in Figure 7 (a & b) The ANOVA Table 8 provides information on the variability between groups and within groups, helping to determine the significance of the factors and their interactions of BTE.

Equation 4 for a Normal Piston and Equation 5 for an Al_2O_3 Coated Piston were derived from the RSM quadratic model of BSFC based on the measured parameters

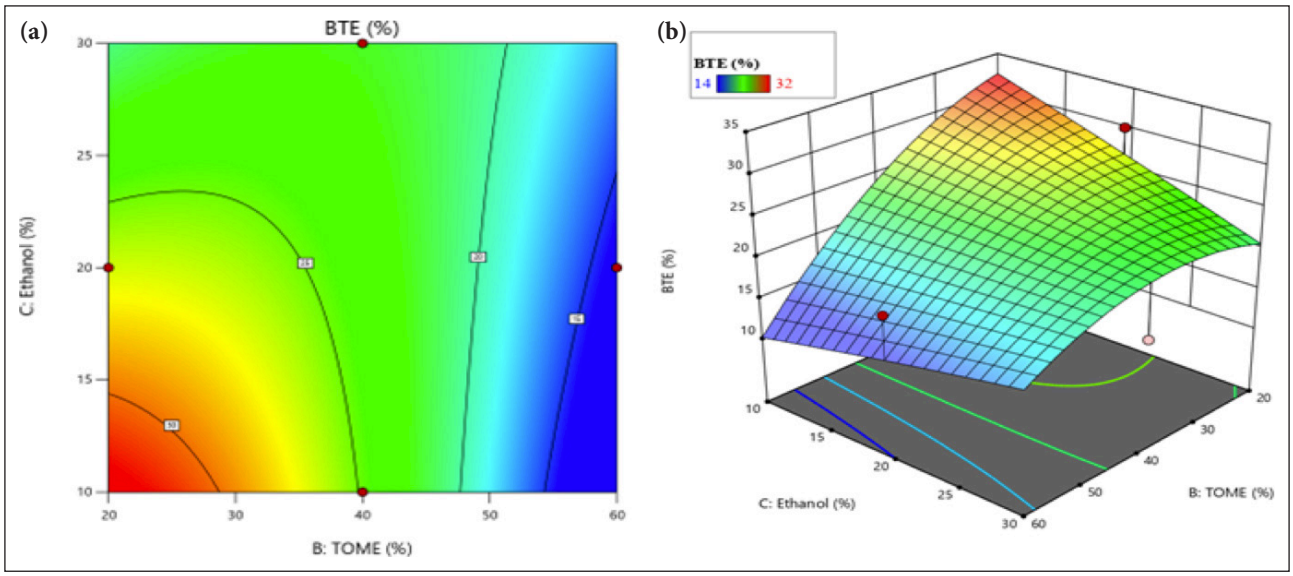

Figure 6. **(a)** 2D and **(b)** 3D Surface plot with load/TOME/ethanol with normal piston – BTE performance.

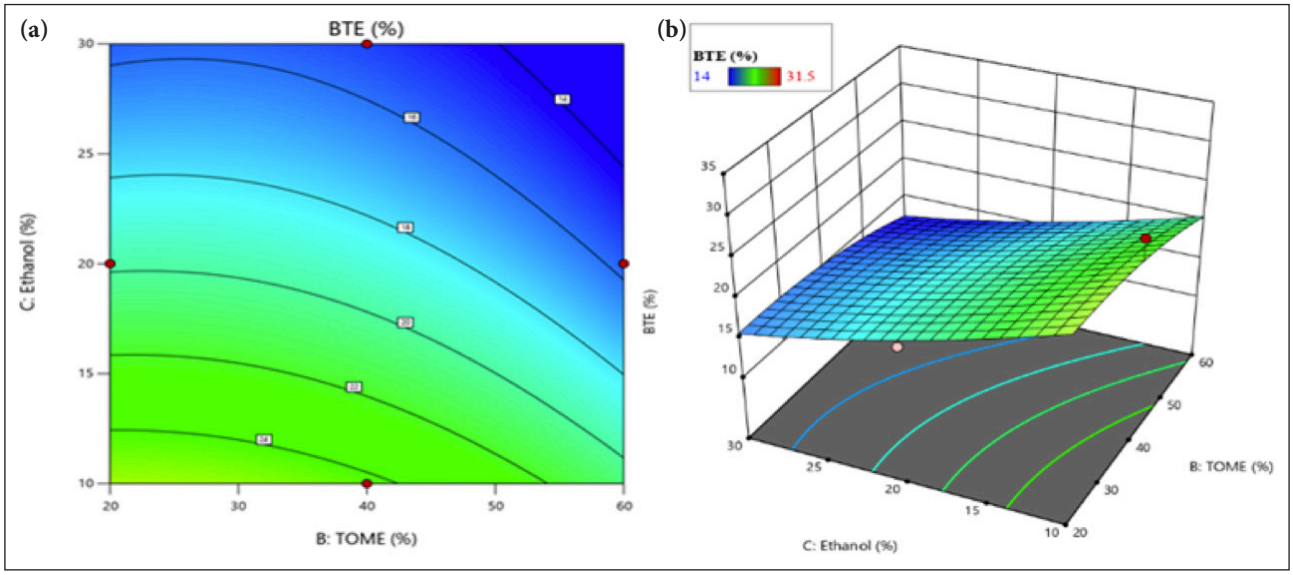

Figure 7. **(a)** 2D and **(b)** 3D Surface plot with Load/TOME/Ethanol with Al2O3 Coated piston – BTE.

[BSFC=0.388+0.07125*A+0.03*B+-0.00625*C+0.0575*AB+0.045*AC+-0.0875*BC+0.136*A^2+0.0935*B^2+-0.109*C^2] (4)

[BSFC=0.468+-0.00375*A+0.05125*B+0.0225*C+-0.02*AB+0.0325*AC+0.1675*BC+-0.0765*A^2+0.1285*B^2+-0.104*C^2] (5)

Figure 8 (a) 2D and (b) 3D surface plot shows the BSFC performance of normal piston, the increase in (BSFC) was qualified to the simultaneous rise in injected fuel and ethanol. Demonstrates that the (BSFC) reduces as the engine load rises when using ethanol ratios. When compared to diesel, B10E20 and B30E20 blends obtained a reduction of 3.6% and 12% in (BSFC), with values of 0.71 kg/kW-h and 0.21 kg/kW-h, respectively. However, B30E20 blends showed an increase of 8% in fuel consumption compared to diesel. Engines running on blends of biodiesel consume a greater amount of fuel than traditional diesel engines do because biodiesel blends have a higher volume and a lower energy content than traditional diesel [28]. The ANOVA Table 9 provides information on the variability between groups and within groups, helping to determine the significance of the factors and their interactions of BSFC. As the biodiesel blend ratio increases, the fuel consumption increases due to the decrease in the amount of energy and the density of the combination of fuels [26]. Due to the excellent heat retention properties of the Al_2O_3 coating, shown in Figure 9 (a & b) it allows for higher temperatures inside the cylinder, leading to improved oxidation of the biodiesel mixture. This, in turn, enhances atomization and vaporization. The B20E10 mix demonstrated a roughly 3.5% improvement compared to pure diesel, but its (BSFC) was higher in comparison to that of the B30E10 blend, resulting in reduced consumption of fuel while maintaining a constant engine speed.

Table 8. Anova parametric results – BTE

	Normal piston			Thermal barrier (Al_2O_3) coated piston		
Source	**Sum of squares**	**F-value**	**p**	**Sum of squares**	**F-value**	**p**
Model	311.88	0.7744	0.6477	361.17	1.30	0.3724
A-load	9.24	0.2066	0.6632	60.50	1.96	0.2040
B-TOME	42.78	0.9561	0.3608	19.53	0.6334	0.4523
C-ethanol	1.20	0.0268	0.8745	16.53	0.5361	0.4878
AB	72.25	1.61	0.2444	1.0000	0.0324	0.8622
AC	3.24	0.0724	0.7956	144.00	4.67	0.0675
BC	85.56	1.91	0.2092	0.5625	0.0182	0.8964
A^2	39.10	0.8739	0.3810	108.98	3.53	0.1022
B^2	52.24	1.17	0.3157	6.19	0.2007	0.6677
C^2	0.1253	0.0028	0.9593	2.61	0.0847	0.7795
Residual	313.23			215.86		
Lack of fit	209.18	2.68	0.1823	34.56	0.2542	0.8552
Pure error	104.05			181.30	1.30	0.3724

TOME: Tomato methyl ester.

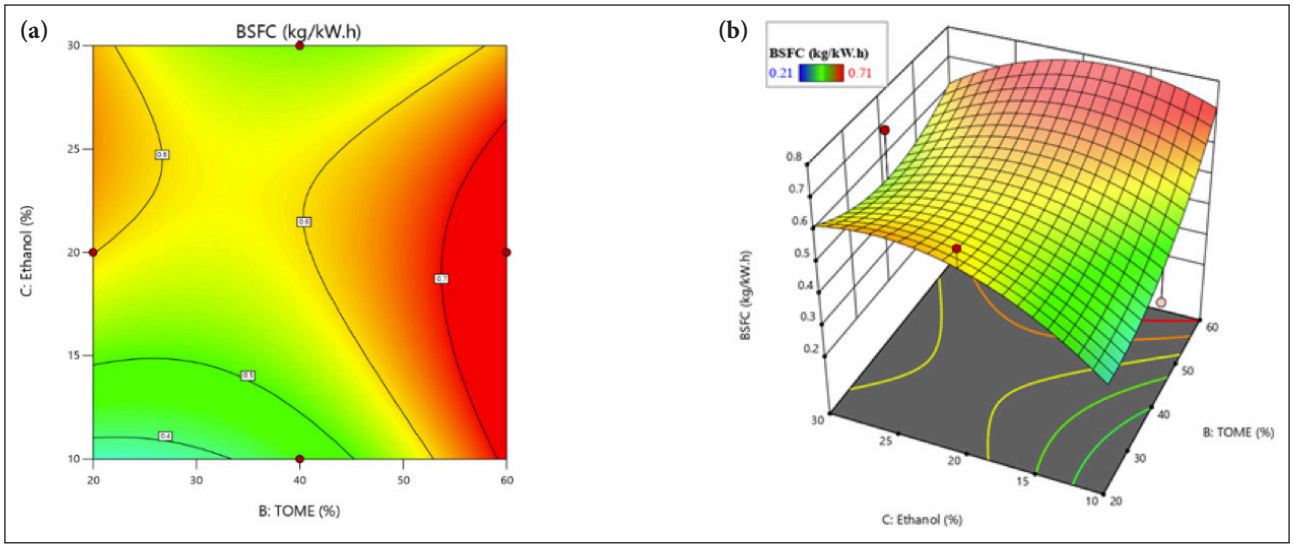

Figure 8. **(a)** 2D and **(b)** 3D surface plot with load/TOME/Ethanol with normal piston – BSFC performance.

Emission Result

Equation 6 for a Normal Piston and Equation 7 for an Al_2O_3 Coated Piston were derived from the RSM quadratic model of CO emission based on the measured parameters.

[CO=0.033+0.00625*A+-0.013125*B+-0.018125*C+0.0175*AB+-0.025*AC+0.01875*BC+0.006625*A^2+0.002875*B^2+-0.004625*C^2] (6)

[CO=0.0684+-0.017375*A+0.002125*B+-0.00825*C+-0.017*AB+0.02225*AC+-0.00225*BC+0.00205*A^2+-0.01745*B^2+-0.0107*C^] (7)

Equation 8 for a Normal Piston and Equation 9 for an Al_2O_3 Coated Piston were derived from the RSM quadratic model of CO emission based on the measured parameters.

[CO=0.033+0.00625*A+-0.013125*B+-0.018125*C+0.0175*AB+-0.025*AC+0.01875*BC+0.006625*A^2+0.002875*B^2+-0.004625*C^2] (8)

[CO=0.0684+-0.017375*A+0.002125*B+-0.00825*C+-0.017*AB+0.02225*AC+-0.00225*BC+0.00205*A^2+-0.01745*B^2+-0.0107*C^] (9)

Figure 10 (a) 2D and (b) 3D surface plot shows the CO emission of normal piston, the emission of (CO) from diesel is reduced when full combustion takes place under low loads. More biodiesel blends are available than diesel, and it has fewer carbon monoxide emissions. As a result of the incorporation of biodiesel into gasoline blends, the researchers discovered that CO and CO_2 emissions were influenced. It is because biodiesel has a greater amount of oxygen. Therefore, carbon monoxide (CO) is decreased, and carbon dioxide (CO_2) is the bigger load mass. This is connected to chemical

Table 9. ANOVA Parametric results – BSFC

	Normal piston			Thermal barrier (Al_2O_3) coated piston		
Source	**Sum of squares**	**F-value**	**Source**	**Sum of squares**	**F-value**	**Source**
Model	0.2600	0.6607	Model	0.2600	0.6607	Model
A-load	0.0406	0.9289	A-load	0.0406	0.9289	A-load
-B-TOME	0.0072	0.1647	-B-TOME	0.0072	0.1647	-B-TOME
C-ethanol	0.0003	0.0071	C-ethanol	0.0003	0.0071	C-ethanol
AB	0.0132	0.3025	AB	0.0132	0.3025	AB
AC	0.0081	0.1853	AC	0.0081	0.1853	AC
BC	0.0306	0.7004	BC	0.0306	0.7004	BC
A^2	0.0779	1.78	A^2	0.0779	1.78	A^2
B^2	0.0368	0.8419	B^2	0.0368	0.8419	B^2
C^2	0.0500	1.14	C^2	0.0500	1.14	C^2
Residual	0.3061		Residual	0.3061		Residual
Lack of fit	0.1968	2.40	Lack of fit	0.1968	2.40	Lack of fit
Pure error	0.1093		Pure error	0.1093		Pure error

BSFC: Brake-specific fuel consumption; TOME: Tomato methyl ester.

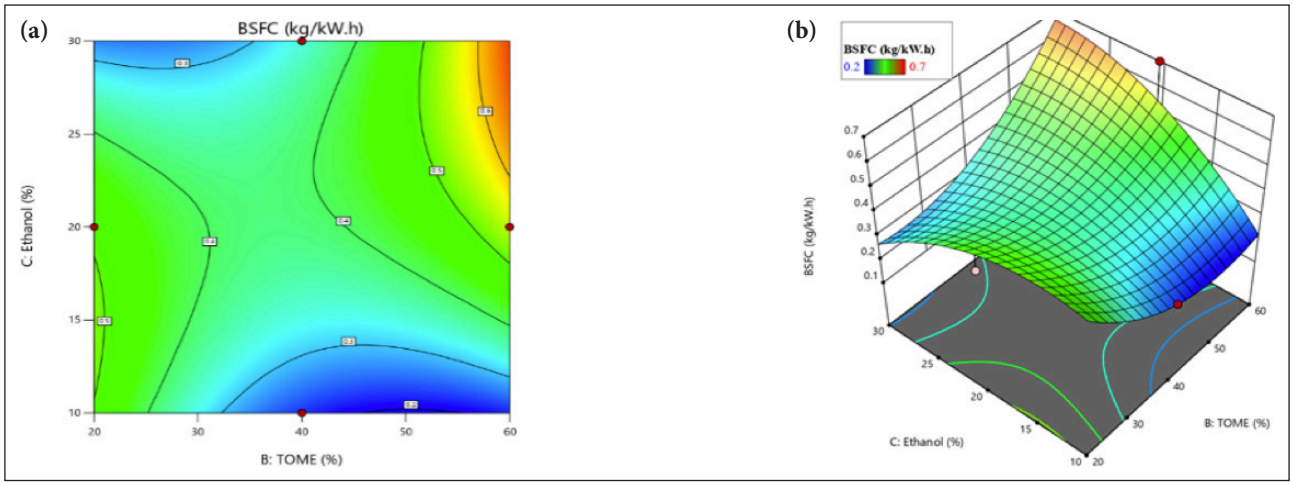

Figure 9. **(a)** 2D and **(b)** 3D surface plot with load/TOME/ethanol with Al_2O_3 coated piston – BSFC performance.

reactions that increase the generation of carbon monoxide [6]. Based on the data presented in Figure 9, it can be observed that B20E20 blends, which have a greater CO emission, and B10E20 blends, which have lower CO emissions by 5.6% and 10.2%, respectively, in comparison to pure diesel, whereas B30 blends produce higher CO emissions than diesel shown in Figure 11 (a & b). In addition, the thermal barrier Al_2O_3 coatings had an effect on carbon monoxide emissions, with coated engines producing a lower level of emissions compared to engines that were not treated. It is through late-phase burning and the subsequent oxidation of carbon monoxide that nanocoated thermal resistance is triggered. The ANOVA Table 10 provides information on the variability between groups and within groups, helping to determine the significance of the factors and their interactions of CO emission. There was a decrease in the amount of carbon monoxide emissions as the speed of the engine increased, and when it was working at its optimal speed, the amount of CO emissions was decreased.

Equation 10 for a Normal Piston and Equation 11 for an Al_2O_3 Coated Piston were derived from the RSM quadratic model of HC emission based on the measured parameters.

[HC=47+-3.375*A+-0.875*B+-2.75*C+5*AB+-2.75*AC+3.25*BC+5*A^2+-3.5*B^2+-1.75*C^2] (10)

[HC=50.28+-4.325*A+-3*B+-1.6*C+-2.05*AB+2*AC+1.85*BC+-2.765*A^2+0.785*B^2+-0.515*C^2] (11)

Figure 12 (a) 2D and (b) 3D surface plot shows the HC emission of normal piston, as a result of the presence of oxygen in ethanol, the oxidation of air hydrocarbons is accelerated, which leads to an improvement in fuel economy. Hydrocarbon (HC) emissions are lowered, which also contributes to the improvement. When opposed to the burning of hydrogen mix, the burning of ethanol results in a lower

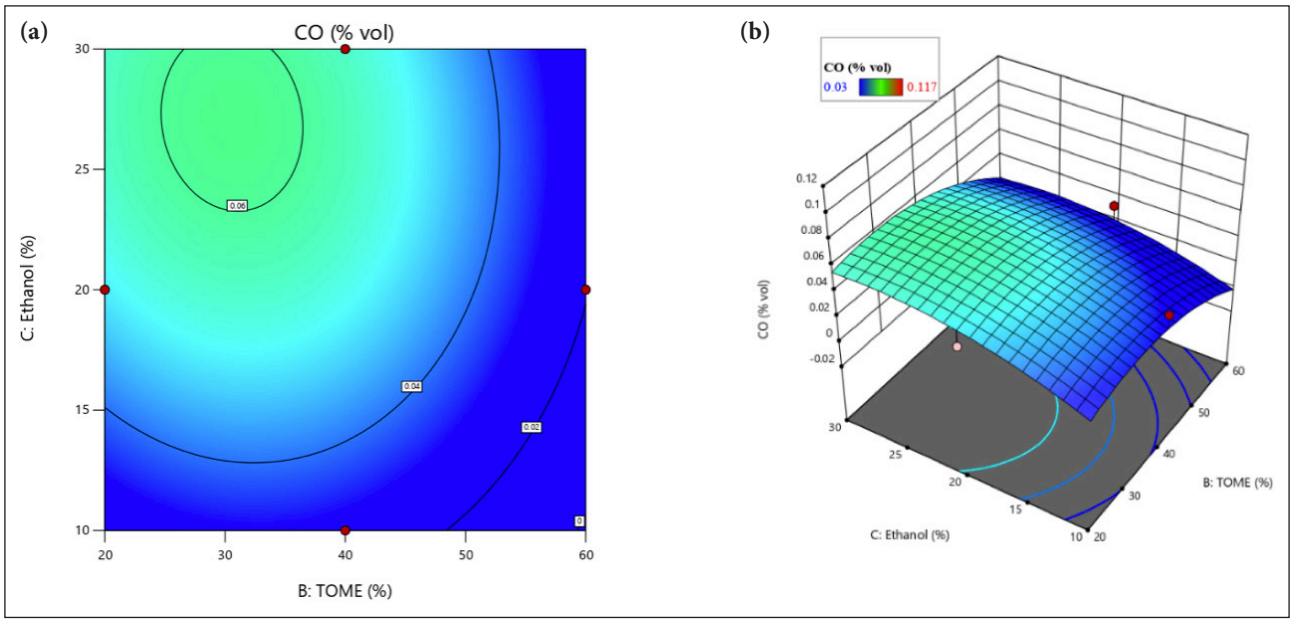

Figure 10. **(a)** 2D and **(b)** 3D Surface plot with load/TOME/ethanol with normal piston – CO emission.

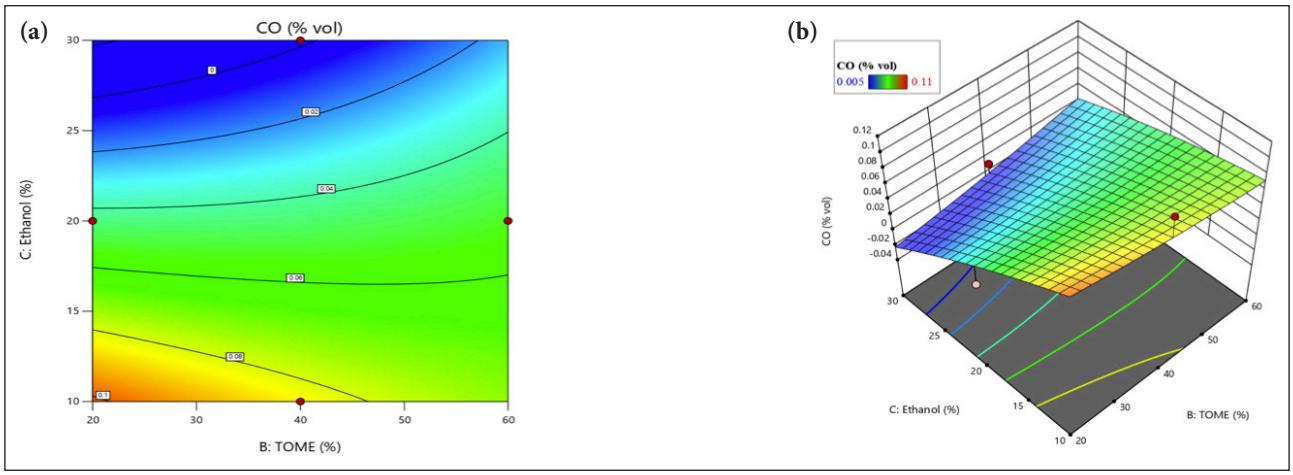

Figure 11. **(a)** 2D and (b) 3D surface plot with load/TOME/ethanol with Al2O3 coated piston – CO emission.

burning temperature and pressure, which leads to a lesser oxidation of hydrocarbons [7]. This is responsible for of the larger HC emissions that are produced. As can be seen in Figure 13, B10E30, which produces higher emissions, and B10E10 blends produce lower hydrocarbon emissions by 3.5% and 10.6%, accordingly, relative to unadulterated diesel. If B10E10 blends are contrasted to diesel, they result in 10.6% more HC. A coated piston and higher temperatures in the engine's combustion area head both contributed to an increase in the pace at which gasoline evaporated. Because of the higher combustion temperature provided by the thermal barrier Al_2O_3 layer, fuel combustion is made easier and more efficient. Because of the enhanced pace at which the thermal barrier coating breaks down hydrocarbons into hydrogen as well as oxygen in the combustion process, coated pistons were found to have lower levels of hydrocarbon emissions as shown in Figure 13(a &b). The ANOVA Table 11 provides information on the variability between groups and within groups, helping to determine the significance of the factors and their interactions of HC emission. It is necessary to take into consideration other parameters, such as quenching range and combustibility threshold, in order to reduce the amount of hydrocarbon emissions that are produced by heat barrier coatings [25].

Equation 12 for a Normal Piston and Equation 13 for an Al_2O_3 Coated Piston were derived from the RSM quadratic model of NoX emission based on the measured parameters.

[NoX=562.6+44.125*A+12.375*B+34.25*C+-108.25*AB+141.5*AC+-104*BC+-54.675*A^2+90.825*B^2+-38.425*C^2] (12)

[NoX=556.3+95.8875*A+47.45*B+45.9875*C+12.7*AB+14.875*AC+-29.65*BC+81.6125*A^2+-79.6625*B^2+23.1125*C^2] (13)

Figure 14 (a) 2D and (b) 3D surface plot shows the NoX emission of normal piston, Lowering the rate at which the premixed fuel is burned reduces the emissions of nitrogen oxide (NoX) while minimizing the release of heat. There is

Table 10. ANOVA parametric results – CO emission

	Normal piston			Thermal barrier (Al_2O_3) coated piston		
Source	**Sum of squares**	**F-value**	**p**	**Sum of squares**	**F-value**	**p**
Model	0.0097	0.9947	0.5149	0.0080	0.8355	0.6085
A-load	0.0003	0.2869	0.6088	0.0024	2.27	0.1758
B-TOME	0.0014	1.27	0.2977	0.0000	0.0339	0.8591
C-ethanol	0.0026	2.41	0.1643	0.0005	0.5114	0.4977
AB	0.0012	1.12	0.3241	0.0012	1.09	0.3320
AC	0.0025	2.30	0.1735	0.0020	1.86	0.2149
BC	0.0014	1.29	0.2932	0.0000	0.0190	0.8942
A^2	0.0002	0.1697	0.6927	0.0000	0.0166	0.9010
B^2	0.0000	0.0320	0.8632	0.0013	1.20	0.3088
C^2	0.0001	0.0827	0.7820	0.0005	0.4528	0.5226
Residual	0.0076			0.0075		
Lack of fit	0.0034	1.10	0.4467	0.0019	0.4664	0.7215
Pure error	0.0042			0.0055	0.8355	0.6085

BSFC: Brake-specific fuel consumption; TOME: Tomato methyl ester.

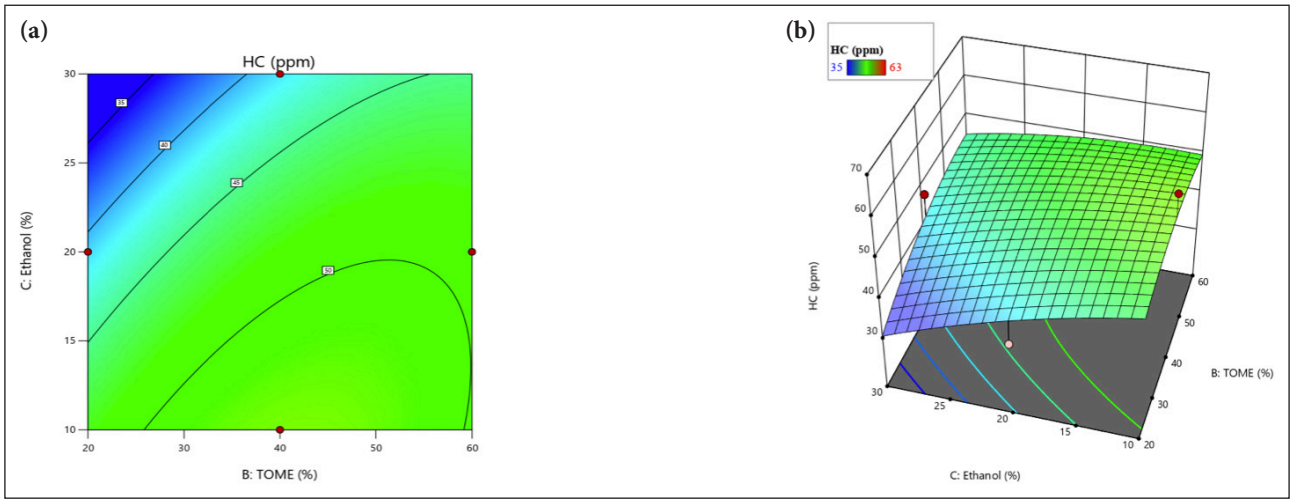

Figure 12. **(a)** 2D and **(b)** 3D surface plot with load/TOME/ethanol with normal piston – HC emission.

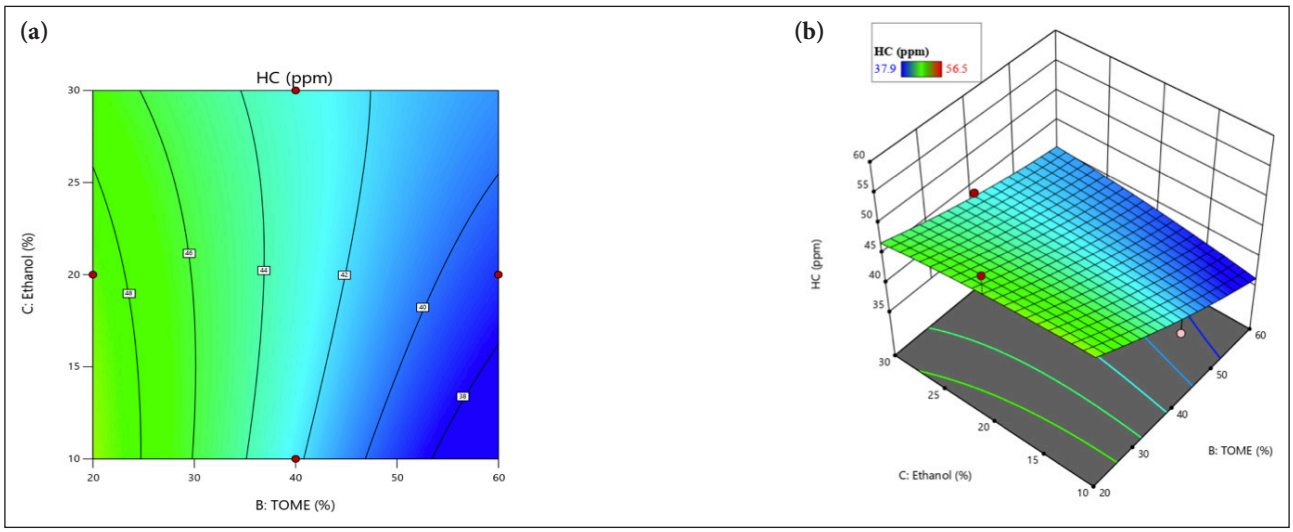

Figure 13. **(a)** 2D and **(b)** 3D surface plot with load/TOME/ethanol with Al2O3 coated piston – HC emission.

Table 11. ANOVA şarametric results – HC emission

	Normal piston			Thermal barrier (Al_2O_3) coated piston		
Source	**Sum of squares**	**F-value**	**p**	**Sum of squares**	**F-value**	**p**
Model	491.51	1.14	0.4396	324.20	1.62	0.2676
A-load	91.13	1.91	0.2096	149.64	6.75	0.0355
B-TOME	6.13	0.1283	0.7308	72.00	3.25	0.1146
C-ethanol	60.50	1.27	0.2974	20.48	0.9236	0.3685
AB	100.00	2.09	0.1911	16.81	0.7581	0.4128
AC	30.25	0.6335	0.4522	16.00	0.7216	0.4237
BC	42.25	0.8848	0.3782	13.69	0.6174	0.4578
A^2	105.26	2.20	0.1812	32.19	1.45	0.2674
B^2	51.58	1.08	0.3332	2.59	0.1170	0.7423
C^2	12.89	0.2700	0.6193	1.12	0.0504	0.8288
Residual	334.25			155.21		
Lack of fit	254.25	4.24	0.0984	57.61	0.7869	0.5606
Pure error	80.00			97.61		

HC: Hydrocarbon; TOME: Tomato methyl ester.

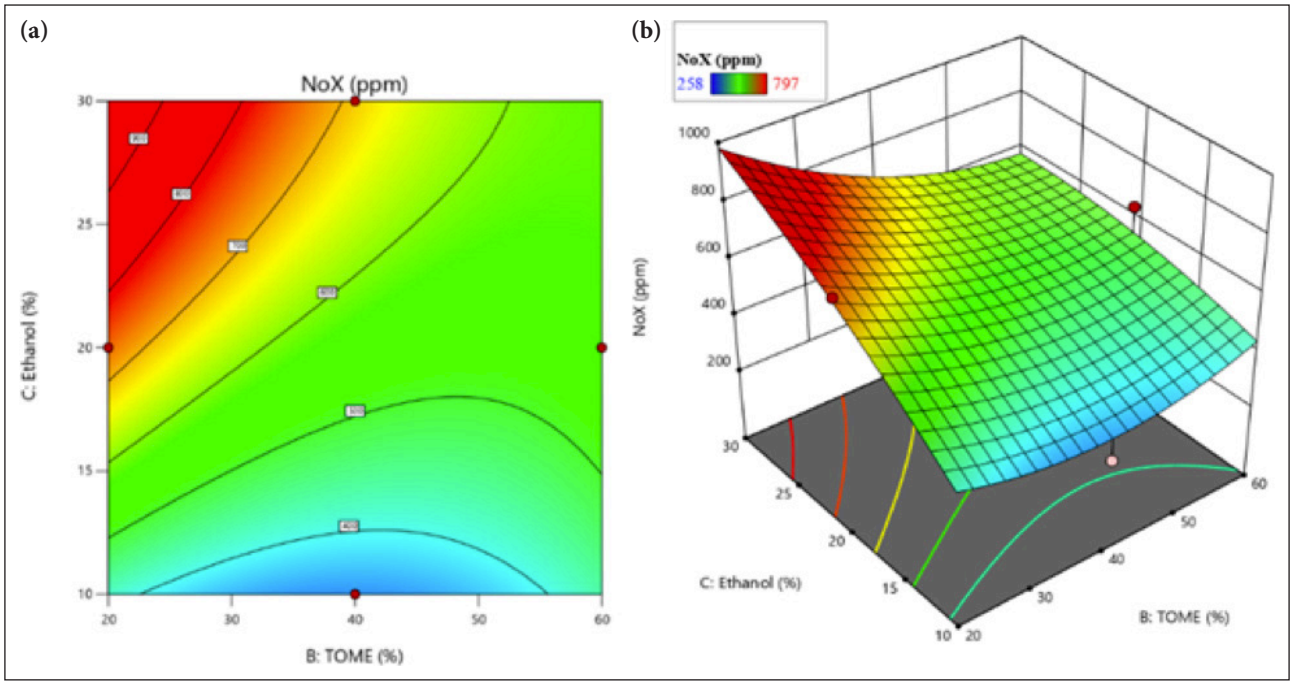

Figure 14. **(a)** 2D and **(b)** 3D surface plot with load/TOME/ethanol with Normal piston – NoX emission.

a correlation between the increase in ethanol's energy contribution and the increase in NOX emissions throughout all states. In ethanol biodiesel dual-fuel engines, the formation of NOX is influenced by a wide variety of parameters. As the temperature of the fire and the rate at which it burns drop, the amount of NOX that is produced increases [1]. Because of a greater use of gasoline, the rise in the strain on the engine was attributed to the increase in the amount of NOX emissions. Blends produce NoX at a rate that is higher than diesel at the highest load conditions, as shown in Figure 13. The rates of production for B20E30, B10E10, and B30E20 blends are 5.5%, 6.5%, and 7.5% respectively. However, there is just one problem that needs to be fixed with the engine that has been coated with Al_2O_3, and that is the emission of NoX. The ANOVA Table 12 provides information on the variability between groups and within groups, helping to determine the significance of the factors and their interactions of NoX. The NO emission of a coated piston engine is greater compared to that of a noncoated piston engine shown in Figure 15 (a & b) and the operating temperature of the coated piston engine may be higher. This combination of factors leads to an earlier start of com-

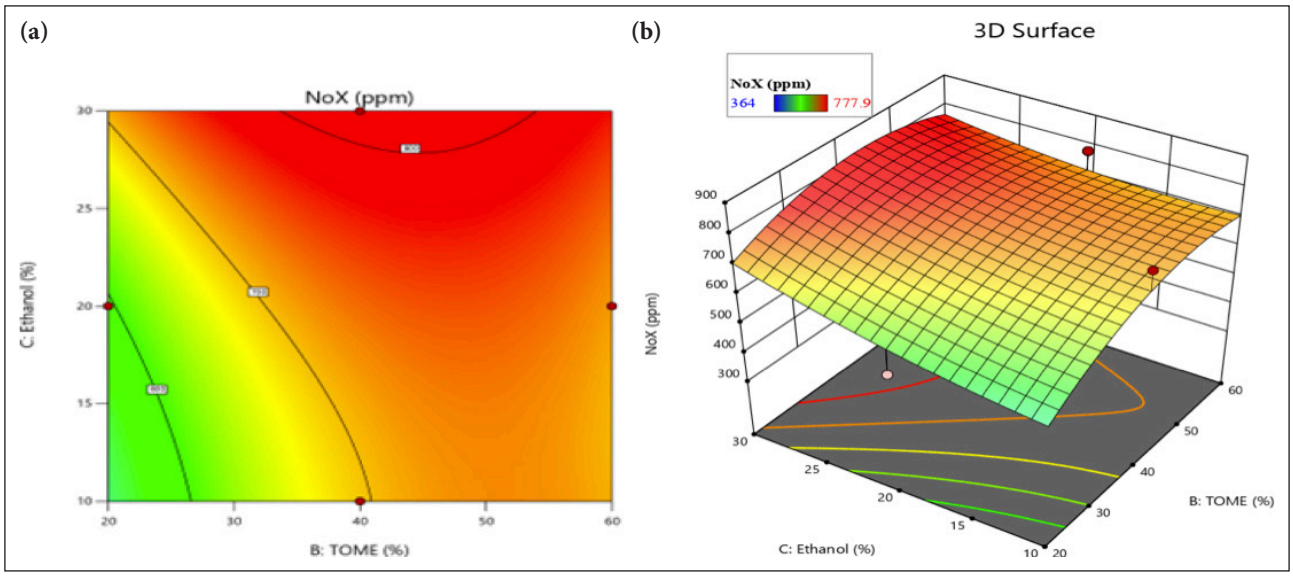

Figure 15. **(a)** 2D and (b) 3D surface plot with load/TOME/ethanol with Al2O3 coated piston – NoX Emission.

Table 12. ANOVA parametric results – NoX emission

	Normal piston			Thermal barrier (Al_2O_3) coated piston		
Source	**Sum of squares**	**F-value**	**p**	**Sum of squares**	**F-value**	**p**
Model	2.473E+05	1.43	0.3249	1.678E+05	0.9702	0.5284
A-load	15576.13	0.8123	0.3974	73555.30	3.83	0.0913
B-TOME	1225.12	0.0639	0.8077	18012.02	0.9370	0.3653
C-ethanol	9384.50	0.4894	0.5068	16918.80	0.8802	0.3794
AB	46872.25	2.44	0.1619	645.16	0.0336	0.8598
AC	80089.00	4.18	0.0803	885.06	0.0460	0.8362
BC	43264.00	2.26	0.1768	3516.49	0.1829	0.6817
A^2	12586.76	0.6564	0.4445	28044.63	1.46	0.2663
B^2	34733.39	1.81	0.2203	26720.48	1.39	0.2769
C^2	6216.76	0.3242	0.5869	2249.21	0.1170	0.7423
Residual	1.342E+05			1.346E+05		
Lack of fit	39692.75	0.5599	0.6693	70548.11	1.47	0.3495
Pure error	94529.20			64009.50		

TOME: Tomato methyl ester.

bustion, which in turn transfers pressure and temperature. During the premixing phase, the majority of premixed biofuels are burned, which results in a reduction in the amount of NOX emissions [10].

Equation 14 for a Normal Piston and Equation 15 for an Al_2O_3 Coated Piston were derived from the RSM quadratic model of Smoke opacity emission based on the measured parameters.

Smoke=[11.48+1.54375*A+1.93125*B+2.15*C+2.3375*AB+4*AC+1.2*BC+-1.93375*A^2+-2.88375*B^2+9.20375*C^2] (14)

Smoke= [21.67+-4.9225*A+0.20375*B+0.10375*C+-6.11*AB+-0.495*AC+-1.3475*BC+0.00875*A^2+-7.66375*B^2+-0.97375*C^2] (15)

Figure 16 (a) 2D and (b) 3D surface plot shows the smoke emission of normal piston, inefficient combustion of the fuel results in the production of smoke. This is because smoke is produced when the fuel is burned. Additionally, as the engine's load grows, the unused energy of evaporation decreases and the ensuing delay in igniting occurs, both of which have an impact on reducing the amount of smoke emissions. By comparing pure diesel to B20E10, which creates greater emissions, and B30E30 blends, which produce reduced smoke emissions by 4.5% and 8.6%, respectively, as shown in Figure 15, it is clear that the former produces higher emissions. The application of an Al_2O_3 coating to engine components results in the production of high burning temperatures shown in Figure

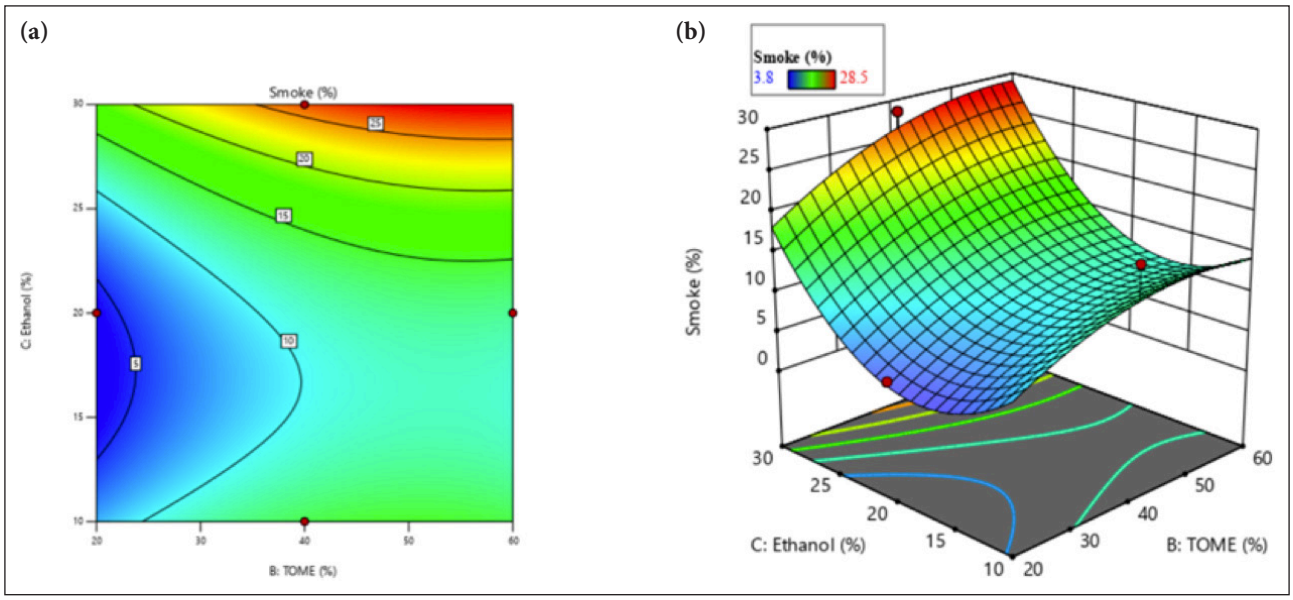

Figure 16. **(a)** 2D and **(b)** 3D surface plot with load/TOME/ethanol with normal piston – smoke opacity.

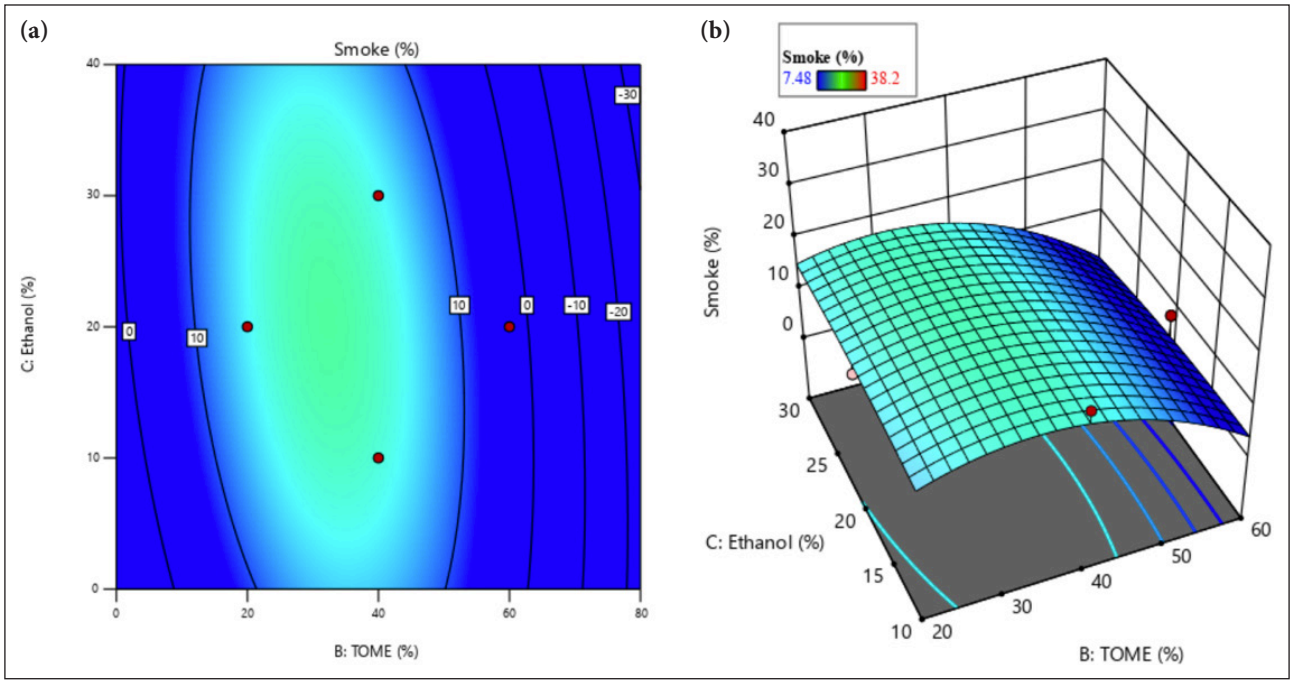

Figure 17. **(a)** 2D and **(b)** 3D surface plot with Load/TOME/ethanol with Al_2O_3 coated piston – Smoke opacity.

17 (a & b) which has the effect of completely consuming the fuel. Because of this, the amount of smoke emissions produced by coated pistons at high ratios of compression is reduced, as evidenced by the fact that [16]. can be recorded. The ANOVA Table 13 provides information on the variability between groups and within groups, helping to determine the significance of the factors and their interactions of Smoke opacity.

CONCLUSION

The (RSM) optimization technique proved to be effective in investigating the influence of load, Tomato Methyl Ester (TOME), and Ethanol injection on engine performance and exhaust gas pollutants.

- The use of thermal barrier coatings, particularly Al_2O_3, on the piston operating with biodiesel blends exhibited potential in enhancing engine performance and minimizing emissions.
- Blends of biodiesel, such as B20E30, B10E20, and B30E20, exhibited comparable performance and emission levels to those of pure diesel. The B20E30 mix displayed a marginal 3.5% reduction in brake thermal efficiency (BTE) in comparison to pure diesel. However, its BTE was inferior to that of the B30E20 blend.

Table 13. ANOVA parametric results – smoke opacity

	Normal piston			Thermal barrier (Al_2O_3) coated piston		
Source	**Sum of squares**	**F-value**	**p**	**Sum of squares**	**F-value**	**p**
Model	569.08	0.8523	0.5979	608.08	0.6445	0.7359
A-Load	19.07	0.2570	0.6278	193.85	1.85	0.2161
B-TOME	29.84	0.4022	0.5461	0.3321	0.0032	0.9567
C-Ethanol	36.98	0.4985	0.5030	0.0861	0.0008	0.9779
AB	21.86	0.2946	0.6041	149.33	1.42	0.2716
AC	64.00	0.8627	0.3839	0.9801	0.0093	0.9257
BC	5.76	0.0776	0.7886	7.26	0.0693	0.8000
A^2	15.74	0.2122	0.6590	0.0003	3.075E-06	0.9986
B^2	35.01	0.4720	0.5142	247.30	2.36	0.1684
C^2	356.67	4.81	0.0644	3.99	0.0381	0.8508
Residual	519.30			733.85		
Lack of Fit	206.45	0.8799	0.5228	195.42	0.4839	0.7113
Pure Error	312.85			538.43	0.6445	0.7359

TOME: Tomato methyl ester.

- Ethanol, when used as a fuel along with a glow plug, decreased polluting emissions from the exhaust. However, it also resulted in lower efficiency compared to diesel fuel.
- Delaying the ethanol injection enhanced the thermal efficiency of the engine and decreased carbon monoxide and unburned hydrocarbon emissions. However, it resulted in higher nitrogen oxide emissions as a result of increased combustion temperatures. The low heat rejection engine, which was fitted with a partially stabilized Al_2O_3 coating, demonstrated a higher thermal efficiency in comparison to alternative engines.
- Ethanol, when used as a fuel with a glow plug, decreases the emission of pollutants from the exhaust. However, it also results in a decrease in efficiency compared to the usage of diesel fuel. Delaying the injection timing of the engine enhances its thermal efficiency to a certain extent, resulting in a reduction in carbon monoxide and unburned hydrocarbon emissions.

ACKNOWLEDGEMENTS

The authors are obliged to Aarupadai Veedu Institute of Technology, Vinayaka Mission's Research Foundation for providing laboratory facilities.

DATA AVAILABILITY STATEMENT

The author confirm that the data that supports the findings of this study are available within the article. Raw data that support the finding of this study are available from the corresponding author, upon reasonable request.

CONFLICT OF INTEREST

The author declared no potential conflicts of interest with respect to the research, authorship, and/or publication of this article.

USE OF AI FOR WRITING ASSISTANCE

Not declared.

ETHICS

There are no ethical issues with the publication of this manuscript.

REFERENCES

[1] A. P. Venkatesh, T. P. Latchoumi, S. Chezhian Babu, K. Balamurugan, S. Ganesan, M. Ruban, and L. Mulugeta, "Multiparametric optimization on influence of ethanol and biodiesel blends on nanocoated engine by full factorial design," Journal of Nanomaterials, Vol. 2022, Article 5350122, 2022. [CrossRef]

[2] A. Bernardo, D. Boeris, A. I. Evins, G. Anichini, and P. E. Stieg, "A combined dual-port endoscope-assisted pre-and retrosigmoid approach to the cerebellopontine angle: An extensive anatomo-surgical study," Neurosurgical Review, Vol. 37, pp. 597–608, 2014. [CrossRef]

[3] H. Solmaz, "A comparative study on the usage of fusel oil and reference fuels in an HCCI engine at different compression ratios," Fuel, Vol. 273, Article 117775, 2020. [CrossRef]

[4] S. Prakash, M. Prabhahar, O. P. Niyas, S. Faris, and C. Vyshnav, "Thermal barrier coating on IC engine piston to improve efficiency using dual fuel," Materials Today: Proceedings, Vol. 33, pp. 919–924, 2020. [CrossRef]

[5] V. Saxena, N. Kumar, and V. K. Saxena, "Multi-objective optimization of modified nanofluid fuel blends at different TiO2 nanoparticle concentration in diesel engine: Experimental assessment and modeling," Applied Energy, Vol. 248, pp. 330–353, 2019. [CrossRef]

[6] B. J. Kalita, and N. Sit, "Optimization of the culture conditions for cellulase production from suitable food waste using fungal strain isolated from different soils," Biomass Conversion and Biorefinery, pp. 1–14, 2023. [CrossRef]

[7] S. Kumar, A. Kumar, A. R. Sharma, and A. Kumar, "Heat transfer correlations on combustion chamber surface of diesel engine experimental work," International Journal of Automotive Science and Technology, Vol. 2(3), pp. 28–35, 2019. [CrossRef]

[8] G. Najafi, B. Ghobadian, T. Yusaf, S. M. S. Ardebili, and R. Mamat, "Optimization of performance and exhaust emission parameters of a SI (spark ignition) engine with gasoline–ethanol blended fuels using response surface methodology," Energy, Vol. 90, pp. 1815–1829, 2015. [CrossRef]

[9] S. Kundu, S. K. Das, and P. Sahoo, "Friction and wear behavior of electroless Ni-PW coating exposed to elevated temperature," Surfaces and Interfaces, Vol. 14, pp. 192–207, 2019. [CrossRef]

[10] S. Yessian, and P. A. Varthanan, "Optimization of performance and emission characteristics of catalytic coated IC engine with biodiesel using grey-taguchi method," Scientific Reports, Vol. 10(1), Article 2129, 2020. [CrossRef]

[11] M. Prabhahar, and K. Rajan, "Performance and combustion characteristics of a diesel engine with titanium oxide coated piston using Pongamia methyl ester," Journal of Mechanical Science and Technology, Vol. 27(5), pp. 1519–1526, 2013. [CrossRef]

[12] S. Ozer, F. Haciyusufoglu, and E. Vural, "Experimental investigation of the effect of the use of nanoparticle additional biodiesel on fuel consumption and exhaust emissions in tractor using a coated engine," Thermal Science, Vol. 27(4) Part B, pp. 3189–3197, 2023. [CrossRef]

[13] I. Uogintė, G. Lujanienė, and K. Mažeika, "Study of Cu (II), Co (II), Ni (II) and Pb (II) removal from aqueous solutions using magnetic Prussian blue nano-sorbent," Journal of Hazardous Materials, Vol. 369, pp. 226–235, 2019. [CrossRef]

[14] B. Vinay, A. K. Singh, and A. K. Yadav, "Optimisation of performance and emission characteristics of CI engine fuelled with Mahua oil methyl ester–diesel blend using response surface methodology," International Journal of Ambient Energy, Vol. 41(6), pp. 674–685, 2020. [CrossRef]

[15] J. D. Mejía, N. Salgado, and C. E. Orrego, "Effect of blends of Diesel and Palm-Castor biodiesels on viscosity, cloud point and flash point," Industrial Crops and Products, Vol. 43, pp. 791–797, 2013. [CrossRef]

[16] H. Venu, and P. Appavu, "Analysis on a thermal barrier coated (TBC) piston in a single cylinder diesel engine powered by Jatropha biodiesel–diesel blends," SN Applied Sciences, Vol. 1(12), p. 1669, 2019. [CrossRef]

[17] Y. J. Yang, S. Aziz, S. M. Mehdi, M. Sajid, S. Jagadeesan, and K. H. Choi, "Highly sensitive flexible human motion sensor based on ZnSnO3/PVDF composite," Journal of Electronic Materials, Vol. 46, pp. 4172–4179, 2017. [CrossRef]

[18] M. Akcay, S. Ozer, and G. Satilmis, "Analytical formulation for diesel engine fueled with fusel oil/diesel blends," Journal of Scientific & Industrial Research, Vol. 81, pp. 712–719, 2022. [CrossRef]

[19] R. Bhagavatha, S. Subrahmaniana, and G. Narendrakumar, "Enhanced removal of Ni (II) from electroplating effluents using herbal biomass as alum substituents," Desalination and Water Treatment, Vol. 244, pp. 241–252, 2021. [CrossRef]

[20] K. Viswanathan, D. Balasubramanian, T. Subramanian, and E. G. Varuvel, "Investigating the combined effect of thermal barrier coating and antioxidants on pine oil in DI diesel engine," Environmental Science and Pollution Research, Vol. 26, pp. 15573–15599, 2019. [CrossRef]

[21] G. A. Miraculas, N. Bose, and R. E. Raj, "Optimization of biofuel blends and compression ratio of a diesel engine fueled with Calophyllum inophyllum oil methyl ester," Arabian Journal for Science and Engineering, Vol. 41, pp. 1723–1733, 2016. [CrossRef]

[22] K. Nanthagopal, R. S. Kishna, A. E. Atabani, A. Ala'a, G. Kumar, and B. Ashok, "A compressive review on the effects of alcohols and nanoparticles as an oxygenated enhancer in compression ignition engine," Energy Conversion and Management, Vol. 203, Article 112244, 2020. [CrossRef]

[23] O. Z. E. Salih, and C. Cenab, "Effects of adding waste oil ethylene glycol butyl ether to diesel fuel," International Journal of Automotive Science and Technology, Vol. 7(4), pp. 279–284, 2023. [CrossRef]

[24] S. Prakash, M. Prabhahar, and M. Saravana Kumar, "Experimental analysis of diesel engine behaviours using biodiesel with different exhaust gas recirculation rates," International Journal of Ambient Energy, Vol. 43(1), pp. 1508–1517, 2022. [CrossRef]

[25] M. R. Saxena and R. K. Maurya, "Optimization of engine operating conditions and investigation of nano-particle emissions from a non-road engine fuelled with butanol/diesel blends," Biofuels, 2017. [CrossRef]

[26] S. Koçyiğit, S. Ozer, S. Çelebi, and U. Demir, "Bio-based solutions for diesel engines: Investigating the effects of propolis additive and ethanol on performance and emissions," Thermal Science and Engineering Progress, Vol. 48, Article 102421, 2024. [CrossRef]

[27] M. Tomar, and N. Kumar, "Influence of nanoadditives on the performance and emission characteristics of a CI engine fuelled with diesel, biodiesel, and blends–a review," Energy Sources, Part A: Recovery, Utilization, and Environmental Effects, Vol. 42(23), pp. 2944–2961, 2020. [CrossRef]

[28] M. K. Parida, H. Joardar, A. K. Rout, I. Routaray, and B. P. Mishra, "Multiple response optimizations to improve performance and reduce emissions of Argemone Mexicana biodiesel-diesel blends in a VCR engine," Applied Thermal Engineering, Vol. 148, pp. 1454–1466, 2019. [CrossRef]